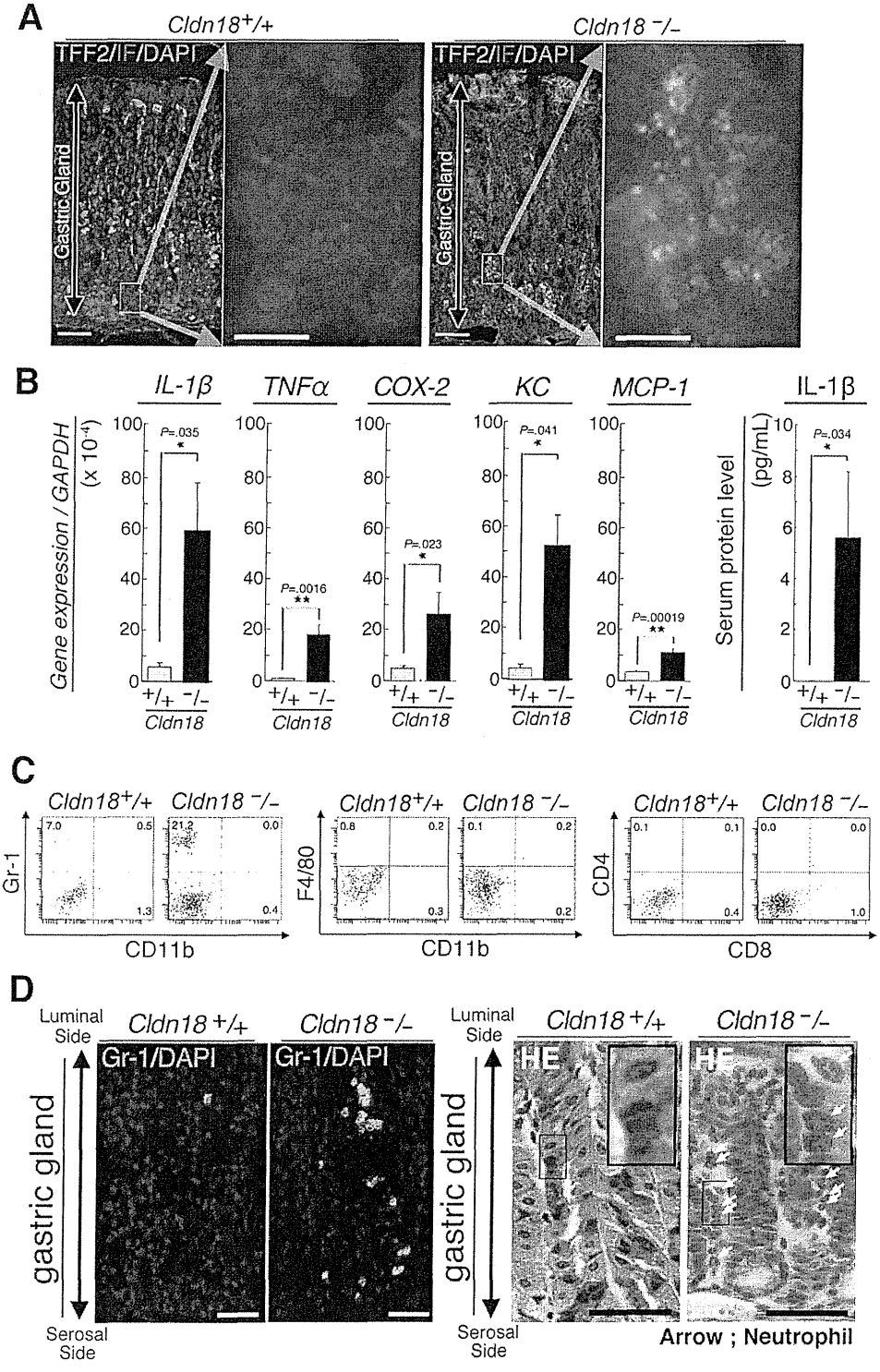

Figure 4. Characterization of the gastritis in *Cldn18*$^{-/-}$ mice. (*A*) Immunofluorescence images of sections stained for TFF2 and IF at low and high magnifications, respectively, in *Cldn18*$^{+/+}$ and *Cldn18*$^{-/-}$ adult stomach. *Bars* = 20 μm. (*B*) Expressions of inflammatory cytokines such as IL-1β, TNF-α, COX2, and KC were up-regulated in *Cldn18*$^{-/-}$ stomach. n ≧ 4. (*C*) Fluorescence-activated cell sorter analysis of immune cell types in gastritic *Cldn18*$^{-/-}$ tissue. Neutrophils, which are positive for Gr-1 and negative for CD11b, were the dominant immune cell type. (*D*) Immunofluorescence micrographs for Gr-1– and H&E-stained micrographs. (*Insets*) High-power micrographs reveal infiltration of neutrophils. *Bars* = 50 μm.

the chronic recruitment of neutrophils and prostaglandin-related reactions.

Effects of Manipulating Gastric Acidity

To obtain additional evidence for or against our interpretation that gastritis in *Cldn18*$^{-/-}$ mice was caused by a paracellular leak of stomach gastric acid, we next examined the effects of administering hydrochloric acid at low concentration or omeprazole sodium, an inhibitor of H^+,K^+-ATPase, on the incidence of gastritis in *Cldn18*$^{+/+}$ and *Cldn18*$^{-/-}$ stomach (Figure 6*B* and *C*).

A low concentration of hydrochloric acid was given to *Cldn18*$^{+/+}$ and *Cldn18*$^{-/-}$ mice on postnatal day 1, when parietal cells have not yet differentiated. Although no

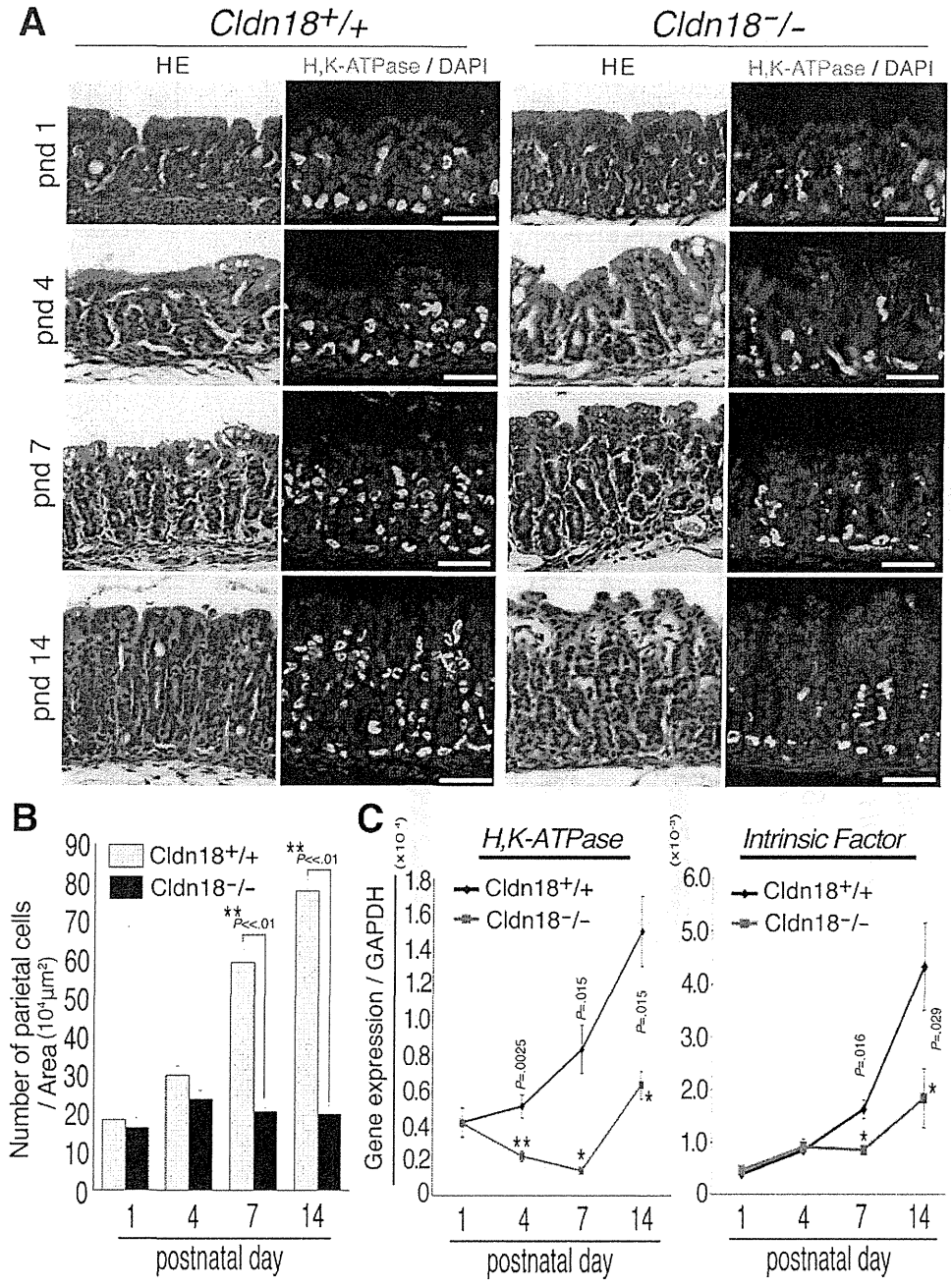

Figure 5. Age-related changes in *Cldn18*$^{+/+}$ and *Cldn18*$^{-/-}$ stomach. (*A*) Light microscopic images of H&E-stained paraffin sections and immunofluorescence micrographs stained for H^+,K^+-ATPase (H,K-ATPase) from *Cldn18*$^{+/+}$ and *Cldn18*$^{-/-}$ stomach at various times after birth. *Bars* = 50 μm. (*B*) Quantification of parietal cell number (shown as numbers per tissue area) in *Cldn18*$^{+/+}$ and *Cldn18*$^{-/-}$ stomach at different ages. (*C*) Gene expression level of markers for the differentiation of gastric cells. n ≧ 4.

inflammation was detected in mice given a neutral buffer, *Cldn18*$^{-/-}$ mice given hydrochloric acid showed stomach inflammation on postnatal day 2, as shown by IL-1β and COX2 levels (Figure 6*B*). When omeprazole was administered for 2 weeks starting at birth (twice a day with 5% dextrose in water), the expression of IL-1β in *Cldn18*$^{-/-}$ mice decreased to ~30% of that in untreated mice (Figure 6*C* [*i*]). The number of parietal cells at postnatal day 14 was significantly recovered by 14-day administration of omeprazole, at least partly indicative of decreased parietal cells after differentiation (Figure 6*C* [*ii*]). However, the induction of gastritis was not blocked, suggesting that omeprazole did not completely inhibit the secretion of gastric acid. These findings further support the idea that stomach acidity in *Cldn18*$^{-/-}$ mice triggers inflammation, which in turn induces gastritis.

Decrease in the Paracellular Barrier Function of Gastric Epithelial Cell Sheets on Claudin-18 Deficiency

We next examined the epithelial paracellular barrier function against H^+ in *Cldn18*$^{+/+}$ and *Cldn18*$^{-/-}$ stomach (Figure 7). Electrophysiologic measurements showed that total conductance was higher in *Cldn18*$^{-/-}$ stomach than *Cldn18*$^{+/+}$ stomach, suggesting that the claudin-18 deficiency resulted in defects in the paracellular barrier. In the

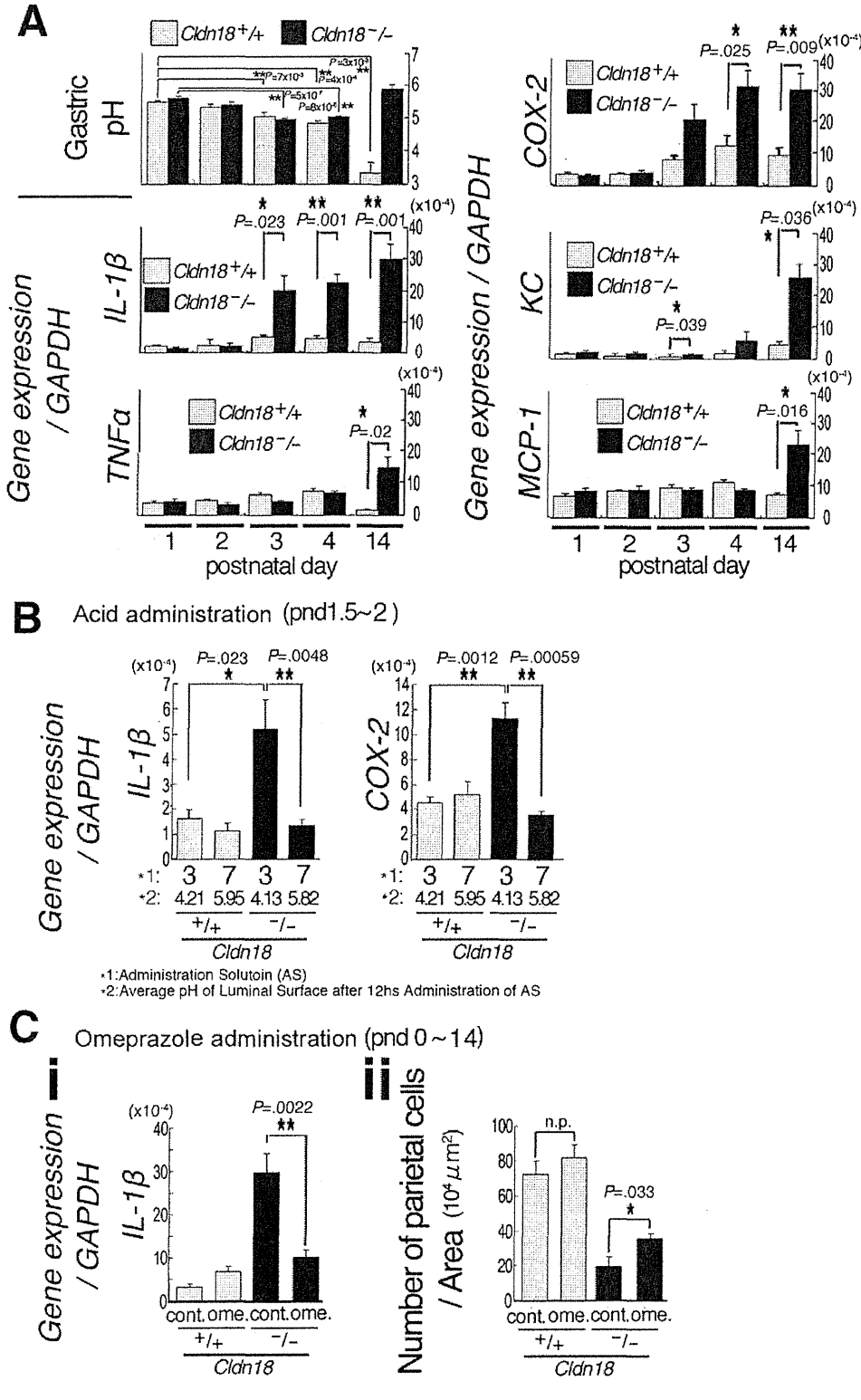

Figure 6. Onset of gastritis in *Cldn18*$^{+/+}$ and *Cldn18*$^{-/-}$ mice. (*A*) Time-dependent changes in pH and expression levels of IL-1β, TNF-α, COX-2, KC, and MCP-1 in untreated *Cldn18*$^{+/+}$ and *Cldn18*$^{-/-}$ mice. n ≧ 4. (*B*) IL-1β and COX-2 were up-regulated after oral administration of acid on postnatal day 1 in *Cldn18*$^{-/-}$ but not *Cldn18*$^{+/+}$ stomach. n ≧ 5. (*C* [*i*]) IL-1β was down-regulated following administration of the proton pump inhibitor omeprazole in *Cldn18*$^{-/-}$ but not *Cldn18*$^{+/+}$ stomach. n ≧ 5. (*C* [*ii*]) Quantification of parietal cell number (shown as numbers per tissue area) in *Cldn18*$^{+/+}$ and *Cldn18*$^{-/-}$ stomach with or without administration of omeprazole. Note that the number is partially recovered by omeprazole.

Cldn18$^{+/+}$ stomach, the paracellular barrier was sensitive to acidity, which caused the conductance to decrease, as shown by the Gt ratio (see Supplementary Materials and Methods) (Figure 7*A*). Consistent with this observation, we detected an H^+ leak by H^+ titration in infant mice, which was quite low in the *Cldn18*$^{+/+}$ stomach compared with the *Cldn18*$^{-/-}$ stomach (Figure 7*A*). In sharp contrast, in the *Cldn18*$^{-/-}$ stomach, the paracellular barrier was not sensitive to the acidity and showed a significantly higher H^+ leak compared with the *Cldn18*$^{+/+}$ stomach, as shown by the net proton flux

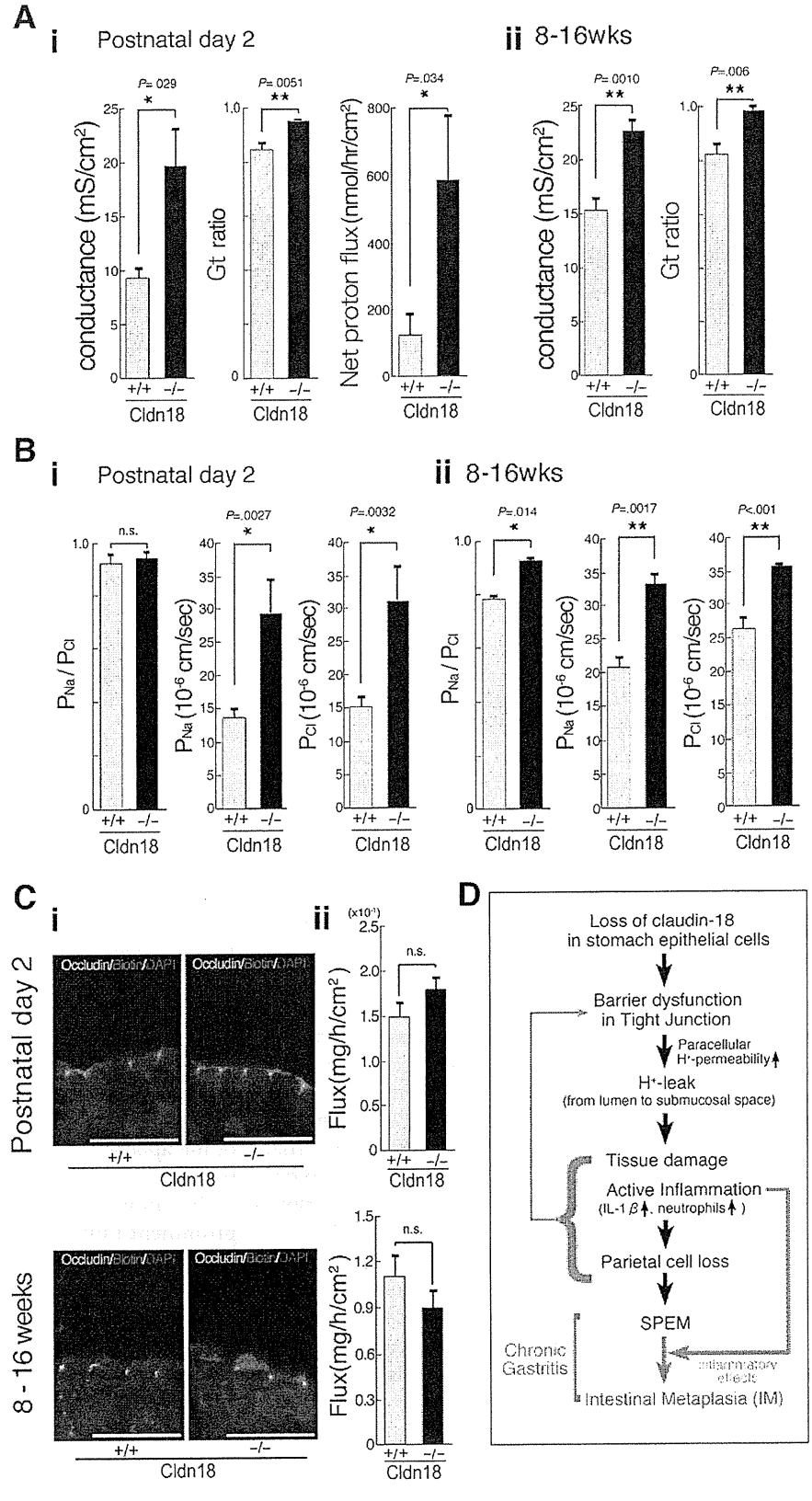

Figure 7. Paracellular permeability of H^+, Na^+, Cl^-, biotin, and dextran. (*A*) Transepithelial conductance and paracellular H^+ permeability at postnatal day 2 and 8–16 weeks in *Cldn18*$^{+/+}$ and *Cldn18*$^{-/-}$ stomach. H^+ permeability was sensitive to the addition of H^+ in *Cldn18*$^{-/-}$ but not in *Cldn18*$^{+/+}$ stomach. n ≧ 4. (*B*) Paracellular permeability of Na^+ and Cl^- in *Cldn18*$^{+/+}$ and *Cldn18*$^{-/-}$ stomach at postnatal day 2 and at 8–16 weeks. n ≧ 4. (*C*) The paracellular barrier to biotin and 4-kilodalton fluorescein isothiocyanate/dextran in *Cldn18*$^{-/-}$ and *Cldn18*$^{+/+}$ stomach in infants (postnatal day 2 of age) and adults (8–16 weeks of age). *Bars* = 20 μm (*D*) Schematic drawing of the pathologic changes of atrophic gastritis in *Cldn18*$^{-/-}$ mice.

(Figure 7*A*). These findings were consistent with the *Cldn18*$^{+/+}$ paracellular barrier in the stomach, providing a specific barrier against H^+ leakage.

On the other hand, dilution potential measurements for NaCl revealed that the paracellular permeability for Na^+ and Cl^- was higher in *Cldn18*$^{-/-}$ mice, even though the ratios of the permeabilities for Na^+ and Cl^- for adult and infant *Cldn18*$^{+/+}$ and *Cldn18*$^{-/-}$ stomachs were similar (0.8–0.95) (Figure 7*B*). Furthermore, no biotin (mol wt, 443 daltons) leakage was detected in either *Cldn18*$^{+/+}$ and *Cldn18*$^{-/-}$ mice, suggesting that pepsin leakage was not a major feature of the *Cldn18*$^{-/-}$-induced gastritis. As a measure of larger-sized molecules permeability, we measured the flux of 4-kilodalton dextran in the stomach of mice at postnatal day 2 and age 8–16 weeks, finding no differences between *Cldn18*$^{-/-}$ and *Cldn18*$^{+/+}$ stomachs (Figure 7*C*). These findings suggested that the *Cldn18*$^{-/-}$ stomach paracellular barrier was generally more leaky for ions than that of *Cldn18*$^{+/+}$ stomach, but not for larger-sized molecules, and that H^+ leakage due to the weak paracellular barrier in *Cldn18*$^{-/-}$ stomach was particularly important for the incidence of gastritis (Figure 7*D*).

Discussion

Atrophic gastritis is generally considered a high-risk condition for gastric cancer because of the accompanying metaplasia and dysplasia. Thus, identifying its causes is an important issue for anticancer therapy as well for maintaining a healthy gastric system. The stomach has several defense mechanisms to protect gastric epithelial tissue from various noxious materials, such as gastric acid and pepsin, and from stimulation by food. An imbalance between protection and insult can lead to gastritis. However, the way in which the TJ achieves its protective function is poorly understood.

A previous report and our present findings show that in atrophic gastritis and gastric cancer, the expression level of stomach-type claudin-18 is significantly decreased in human tissue, implicating claudin-18, directly or indirectly, in these pathological changes.[40] Our *Cldn18*$^{-/-}$ mice described here made a novel model of gastritis that can show the specific role of claudin-18 in the physiology and pathology of stomach epithelial barrier functions (Figure 7).

Of the two types of claudin-18, lung type and stomach type, stomach-type claudin-18 is the predominantly expressed variant in the stomach. Our present findings suggest paracellular barrier leakage of H^+ may be the primary cause of gastritis in *Cldn18*$^{-/-}$ mice. Additionally, in *Cldn18*$^{-/-}$ mice stomach, claudin-2 expression was slightly up-regulated and the Na^+ gradient facilitated Na^+ ions to pass from the submucosa to the gastric luminal space. As a result, H^+ could easily permeate the opposite direction. This H^+ leakage was associated with the up-regulation of proinflammatory cytokines, including IL-1β and COX-2, in our acid administration experiments and over the time course of development of gastritis, although the causal relationship between H^+ leakage and parietal cell differentiation could not be fully established.

There was also a slight change in gastric luminal pH due to a substantial change in the H^+ concentration. This led to metaplasia, an effect that omeprazole could partially inhibit. Other reports on metaplasia in the context of gastritis that have used *Helicobacter felis*–infected mice, histamine receptor knockout mice, occludin knockout mice, and Ménétrier disease models of transforming growth factor α overexpression mice indicate that it may be, at least partly, related to defects in barrier functions, although no direct association was shown.[42–44] In this respect, the expression level of occludin decreased in the superficial mucous epithelial cells of adult but not infant *Cldn18*$^{-/-}$ stomach, suggesting the possibility that the decreased expression of occludin may not contribute to the onset of gastritis but does contribute to its progression in *Cldn18*$^{-/-}$ stomach. Although the tissue differentiation caused by metaplasia is sensitive to numerous factors such as DMP-777, Hip1r KO, KLF4 KO, RUNX3 KO, K19-C2mE, and amphiregulin,[45–49] this report is the first to show a role for tight junctional claudins.

Although the level of IL-1β was significantly lower in *Cldn18*$^{-/-}$ mice seen here than in IL-1β transgenic mice from another study, it may still have been sufficient to trigger inflammation.[50] In those IL-1β–expressing transgenic mice, gastritis progresses to gastric cancer and splenectasis, which we did not detect at least in <20 weeks old *Cldn18*$^{-/-}$ mice. Considering that the rate of gastric cancer in the IL-1β–expressing transgenic mice depends on their IL-1β level, the absence of gastric cancer in our *Cldn18*$^{-/-}$ mice may be owing to the relatively low level of IL-1β. In addition, it was reported that transgenic mice expressing both COX-2 and prostaglandin E synthase 1 develop hyperplastic gastric tumors in which TNF-α plays an important role.[49] We then suggest that the down-regulation of claudin-18 leads to the basic conditions required for the progression of metaplasia. For dysplasia and neoplasia to occur in our *Cldn18*$^{-/-}$ mice, an additional risk factor that increases the level of cytokines such as IL-1β, COX-2, or TNF-α is needed. Future studies of metaplasia in *Cldn18*$^{-/-}$ mice should resolve this question.

The immune response in *Cldn18*$^{-/-}$ mice involves prominent infiltration of neutrophils into the inflamed regions. Given that IL-2, IL-4, and IL-6 were not up-regulated in these mice, however, T cells and B cells are probably not involved in the observed gastritis. The chronic recruitment of neutrophils in the *Cldn18*$^{-/-}$-related gastritis is in sharp contrast to the immune cell behavior in *H pylori*–induced and nonsteroidal anti-inflammatory drug–induced gastritis, in which the levels of biomarkers for Th1 cells, macrophages, and neutrophils all increased.[13,51] Therefore, it is possible that if the decreased claudin-18 level were combined with an additional risk factor that recruits T cells and B cells, the risk of dysplasia and neoplasia might increase greatly.

The role of paracellular barrier-forming claudins in inflammation is particularly noteworthy, because paracellular H^+ leakage may play a role in other kinds of chronic gastritis, including *H pylori*-induced gastritis. Along these lines, the loss of JAM-A, a TJ component, was reported to induce paracellular permeability and an increased susceptibility to dextran sulfate sodium–induced colitis.[52,53] Similar abnormalities are associated with other insults to paracellular barrier function. Because the paracellular barrier shows great variability in its molecular constitution and barrier function, multiple molecular mechanisms can probably lead to inflammation under a variety of conditions. Here we show that claudin-18–dependent formation of the paracellular barrier against H^+ diffusion is likely to play a specific role in prevention of gastritis. As more studies on claudin knockout mice are published, better understanding of its specific physiologic and pathologic functions, especially with regard to inflammation, will emerge, potentially leading to new therapeutic strategies against epithelial barrier–related diseases.

Supplementary Material

Note: To access the supplementary material accompanying this article, visit the online version of *Gastroenterology* at www.gastrojournal.org, and at doi: 10.1053/j.gastro.2011.10.040.

References

1. Cario E. Heads up! How the intestinal epithelium safeguards mucosal barrier immunity through the inflammasome and beyond. Curr Opin Gastroenterol 2010;26:583–590.
2. Marchiando AM, Graham WV, Turner JR. Epithelial barriers in homeostasis and disease. Annu Rev Pathol 2010;5:119–144.
3. Tsukita S, Furuse M, Itoh M. Multifunctional strands in tight junctions. Nat Rev Mol Cell Biol 2001;2:285–293.
4. Van Itallie CM, Anderson JM. Claudins and epithelial paracellular transport. Annu Rev Physiol 2006;68:403–429.
5. Gupta IR, Ryan AK. Claudins: unlocking the code to tight junction function during embryogenesis and in disease. Clin Genet 2010; 77:314–325.
6. Powell DW. Barrier function of epithelia. Am J Physiol 1981;241: G275–G288.
7. Claude P, Goodenough DA. Fracture faces of zonulae occludentes from "tight" and "leaky" epithelia. J Cell Biol 1973;58:390–400.
8. Laine L, Takeuchi K, Tarnawski A. Gastric mucosal defense and cytoprotection: bench to bedside. Gastroenterology 2008;135: 41–60.
9. Weis VG, Goldenring JR. Current understanding of SPEM and its standing in the preneoplastic process. Gastric Cancer 2009;12: 189–197.
10. Mills JC, Shivdasani RA. Gastric epithelial stem cells. Gastroenterology 2011;140:412–424.
11. Ohnishi N, Yuasa H, Tanaka S, et al. Transgenic expression of Helicobacter pylori CagA induces gastrointestinal and hematopoietic neoplasms in mouse. Proc Natl Acad Sci U S A 2008;105: 1003–1008.
12. Srivastava A, Lauwers GY. Pathology of non-infective gastritis. Histopathology 2007;50:15–29.
13. Becker JC, Domschke W, Pohle T. Current approaches to prevent NSAID-induced gastropathy—COX selectivity and beyond. Br J Clin Pharmacol 2004;58:587–600.
14. Oshima H, Hioki K, Popivanova BK, et al. Prostaglandin E_2 signaling and bacterial infection recruit tumor-promoting macrophages to mouse gastric tumors. Gastroenterology 2011;140:596–607.
15. Ishihara S, Fukuda R, Fukumoto S. Cytokine gene expression in the gastric mucosa: its role in chronic gastritis. J Gastroenterol 1996;31:485–490.
16. Lin WW, Karin M. A cytokine-mediated link between innate immunity, inflammation, and cancer. J Clin Invest 2007;117:1175–1183.
17. Sanders MJ, Ayalon A, Roll M, et al. The apical surface of canine chief cell monolayers resists H+ back-diffusion. Nature 1985; 313:52–54.
18. Chen MC, Chang A, Buhl T, et al. Apical acidification induces paracellular injury in canine gastric mucosal monolayers. Am J Physiol 1994;267:G1012–G1020.
19. Jovov B, Van Itallie CM, Shaheen NJ, et al. Claudin-18: a dominant tight junction protein in Barrett's esophagus and likely contributor to its acid resistance. Am J Physiol Gastrointest Liver Physiol 2007;293:G1106–G1113.
20. Madara JL. Regulation of the movement of solutes across tight junctions. Annu Rev Physiol 1998;60:143–159.
21. Umeda K, Ikenouchi J, Katahira-Tayama S, et al. ZO-1 and ZO-2 independently determine where claudins are polymerized in tight-junction strand formation. Cell 2006;126:741–754.
22. Guillemot L, Paschoud S, Pulimeno P, et al. The cytoplasmic plaque of tight junctions: a scaffolding and signalling center. Biochim Biophys Acta 2008;1778:601–613.
23. Balda MS, Matter K. Tight junctions and the regulation of gene expression. Biochim Biophys Acta 2009;1788:761–767.
24. Bauer HC, Traweger A, Zweimueller-Mayer J, et al. New aspects of the molecular constituents of tissue barriers. J Neural Transm 2011;118:7–21.
25. Furuse M, Fujita K, Hiiragi T, et al. Claudin-1 and -2: novel integral membrane proteins localizing at tight junctions with no sequence similarity to occludin. J Cell Biol 1998;141:1539–1550.
26. Van Itallie CM, Fanning AS, Anderson JM. Reversal of charge selectivity in cation or anion-selective epithelial lines by expression of different claudins. Am J Physiol Renal Physiol 2003;285: F1078–F1084.
27. Mineta K, Yamamoto Y, Yamazaki Y, et al. Predicted expansion of the claudin multigene family. FEBS Lett 2011;585:606–612.
28. Simon DB, Lu Y, Choate KA, et al. Paracellin-1, a renal tight junction protein required for paracellular Mg2+ resorption. Science 1999;285:103–106.
29. Muto S, Hata M, Taniguchi J, et al. Claudin-2-deficient mice are defective in the leaky and cation-selective paracellular permeability properties of renal proximal tubules. Proc Natl Acad Sci U S A 2010;107:8011–8016.
30. Tamura A, Hayashi H, Imasato M, et al. Loss of claudin-15, but not claudin-2, causes Na+ deficiency and glucose malabsorption in mouse small intestine. Gastroenterology 2011;140:913–923.
31. Morita K, Furuse M, Fujimoto K, et al. Claudin multigene family encoding four-transmembrane domain protein components of tight junction strands. Proc Natl Acad Sci U S A 1999;96:511–516.
32. Niimi T, Nagashima K, Ward JM, et al. Claudin-18, a novel downstream target gene for the T/EBP/NKX2.1 homeodomain transcription factor, encodes lung- and stomach-specific isoforms through alternative splicing. Mol Cell Biol 2001;21:7380–7390.
33. Tamura A, Kitano Y, Hata M, et al. Megaintestine in claudin-15-deficient mice. Gastroenterology 2008;134:523–534.
34. Tamura A, Kikuchi S, Hata M, et al. Achlorhydria by ezrin knockdown: defects in the formation/expansion of apical canaliculi in gastric parietal cells. J Cell Biol 2005;169:21–28.
35. Matsubayashi M, Ando H, Kimata I, et al. Effect of low pH on the morphology and viability of Cryptosporidium andersoni sporozoites and histopathology in the stomachs of infected mice. Int J Parasitol 2011;41:287–292.

36. Shao J, Sartor RB, Dial E, et al. Expression of intrinsic factor in rat and murine gastric mucosal cell lineages is modified by inflammation. Am J Pathol 2000;157:1197–1205.
37. Huh WJ, Esen E, Geahlen JH, et al. XBP1 controls maturation of gastric zymogenic cells by induction of MIST1 and expansion of the rough endoplasmic reticulum. Gastroenterology 2010;139:2038–2049.
38. Angelow S, Kim KJ, Yu AS. Claudin-8 modulates paracellular permeability to acidic and basic ions in MDCK II cells. J Physiol 2006;571:15–26.
39. Drakes ML, Czinn SJ, Blanchard TG. Regulation of murine dendritic cell immune responses by Helicobacter felis antigen. Infect Immun 2006;74:4624–4633.
40. Sanada Y, Oue N, Mitani Y, et al. Down-regulation of the claudin-18 gene, identified through serial analysis of gene expression data analysis, in gastric cancer with an intestinal phenotype. J Pathol 2006;208:633–642.
41. Nozaki K, Ogawa M, Williams JA, et al. A molecular signature of gastric metaplasia arising in response to acute parietal cell loss. Gastroenterology 2008;134:511–522.
42. Takagi H, Jhappan C, Sharp R, et al. Hypertrophic gastropathy resembling Ménétrier's disease in transgenic mice overexpressing transforming growth factor alpha in the stomach. J Clin Invest 1992;90:1161–1167.
43. Ogawa T, Maeda K, Tonai S, et al. Utilization of knockout mice to examine the potential role of gastric histamine H2-receptors in Menetrier's disease. J Pharmacol Sci 2003;91:61–70.
44. Saitou M, Furuse M, Sasaki H, et al. Complex phenotype of mice lacking occludin, a component of tight junction strands. Mol Biol Cell 2000;11:4131–4142.
45. Goldenring JR, Nomura S. Differentiation of the gastric mucosa III. Animal models of oxyntic atrophy and metaplasia. Am J Physiol Gastrointest Liver Physiol 2006:G999–G1004.
46. Keeley TM, Samuelson LC. Cytodifferentiation of the postnatal mouse stomach in normal and Huntingtin-interacting protein 1-related-deficient mice. Am J Physiol Gastrointest Liver Physiol 2010; 299:G1241–G1251.
47. Li QL, Ito K, Sakakura C, et al. Causal relationship between the loss of RUNX3 expression and gastric cancer. Cell 2002;109:113–124.
48. Nam KT, Lee HJ, Mok H, et al. Amphiregulin-deficient mice develop spasmolytic polypeptide expressing metaplasia and intestinal metaplasia. Gastroenterology 2009;136:1288–1296.
49. Oshima M, Oshima H, Matsunaga A, et al. Hyperplastic gastric tumors with spasmolytic polypeptide-expressing metaplasia caused by tumor necrosis factor-alpha-dependent inflammation in cyclooxygenase-2/microsomal prostaglandin E synthase-1 transgenic mice. Cancer Res 2005;65:9147–9151.
50. Tu S, Bhagat G, Cui G, et al. Overexpression of interleukin-1beta induces gastric inflammation and cancer and mobilizes myeloid-derived suppressor cells in mice. Cancer Cell 2008;14:408–419.
51. Amedei A, Cappon A, Codolo G, et al. The neutrophil-activating protein of Helicobacter pylori promotes Th1 immune responses. J Clin Invest 2006;116:1092–1101.
52. Laukoetter MG, Nava P, Lee WY, et al. JAM-A regulates permeability and inflammation in the intestine in vivo. J Exp Med 2007; 204:3067–3076.
53. Vetrano S, Rescigno M, Cera MR, et al. Unique role of junctional adhesion molecule-a in maintaining mucosal homeostasis in inflammatory bowel disease. Gastroenterology 2008; 135:173–184.

Received June 28, 2011. Accepted October 26, 2011.

Reprint requests

Address requests for reprints to: Sachiko Tsukita, PhD, Laboratory of Biological Science, Graduate School of Frontier Biosciences, Osaka University, 2-2 Yamadaoka, Suita, Osaka 565-0871, Japan. e-mail: atsukita@biosci.med.osaka-u.ac.jp; fax: (81) 6-6879-3329.

Acknowledgments

D.H. and A.T. contributed equally to this report.

The authors thank Drs J. Mills, D. Alpers, and M.Takeichi for their generous gifts of the antibodies; Drs M. Hatakeyama, T. Noda, E. Morii, and K. Aozasa for their helpful discussions; Dr M. Okabe and Ms K. Kawata for generating the claudin-18 knockout mice; Ms Hagiwara for technical assistance; and members of our laboratory for helpful discussion.

Conflicts of interest

The authors disclose no conflicts.

Funding

Supported in part by a Grant-in-Aid for Creative Scientific Research from the Ministry of Education, Science and Culture of Japan (to S.T.).

Ann Surg Oncol (2012) 19:1902–1910
DOI 10.1245/s10434-011-2175-4

Annals of
SURGICAL ONCOLOGY
OFFICIAL JOURNAL OF THE SOCIETY OF SURGICAL ONCOLOGY

ORIGINAL ARTICLE – THORACIC ONCOLOGY

Cytokeratin 7 is a Predictive Marker for Survival in Patients with Esophageal Squamous Cell Carcinoma

Naohide Oue, MD, PhD[1], Tsuyoshi Noguchi, MD, PhD[2], Katsuhiro Anami, MD, PhD[1], Seigo Kitano, MD, PhD[3], Naoya Sakamoto, MD, PhD[1], Kazuhiro Sentani, MD, PhD[1], Naohiro Uraoka, MD[1], Kazuhiko Aoyagi, PhD[4], Teruhiko Yoshida, MD[4], Hiroki Sasaki, PhD[4], and Wataru Yasui, MD, PhD[1]

[1]Department of Molecular Pathology, Hiroshima University Graduate School of Biomedical Sciences, Hiroshima, Japan; [2]Center for Community Medicine, Division of Surgery, Oita University Faculty of Medicine, Yufu, Japan; [3]Department of Surgery I, Oita University Faculty of Medicine, Yufu, Japan; [4]Division of Genetics, National Cancer Center Research Institute, Tokyo, Japan

ABSTRACT

Background. Patients diagnosed with stage II and III esophageal squamous cell carcinoma (ESCC) have variable prognosis. This group would benefit greatly from the discovery of prognostic markers that are capable of identifying individuals for whom adjuvant treatment would be advantageous. The aim of this study was to investigate the impact of immunohistochemically detected cytokeratin 7 (CK7) expression on disease-free survival, overall survival (OS), or therapeutic outcome in patients with ESCC.

Methods. Immunohistochemical analysis of CK7 was performed on 225 surgically resected specimens of stage 0–III ESCC.

Results. In total, 20 (9%) of 225 ESCC cases were positive for CK7. In stage 0–III ESCC patients, CK7 expression was statistically significantly associated with OS, independent of clinical covariates, including tumor, node, metastasis system stage. In stage II and III ESCC patients ($n = 124$), CK7 expression was significantly associated with poorer OS ($P = 0.0377$). Furthermore, in stage II and III ESCC patients who did not receive adjuvant chemotherapy ($n = 73$), CK7 expression was significantly associated with poorer OS ($P = 0.0003$). CK7 expression was not associated with therapeutic outcome in patients with stage II and III ESCC who received adjuvant chemotherapy. In patients with CK7-positive ESCC ($n = 16$), receipt of adjuvant chemotherapy tended to be beneficial for patients with stage II and III ESCC ($P = 0.0654$).

Conclusions. Immunohistochemical analysis of CK7 will help to identify high-risk patients.

Electronic supplementary material The online version of this article (doi:10.1245/s10434-011-2175-4) contains supplementary material, which is available to authorized users.

First Received: 19 July 2011;
Published Online: 28 December 2011

W. Yasui, MD, PhD
e-mail: wyasui@hiroshima-u.ac.jp

According to the World Health Organization, esophageal cancer is the sixth most common malignancy worldwide.[1] The two predominant forms of esophageal cancer are squamous cell carcinoma and adenocarcinoma. Globally, squamous cell carcinoma accounts for more than 90% of esophageal cancer. Most esophageal squamous cell carcinoma (ESCC) is diagnosed at an advanced stage, and even superficial ESCC that appears to extend no further than the submucosa metastasizes to the lymph nodes in 50% of cases.[2] For localized ESCC, surgery is the primary therapeutic option. However, the prognosis is unsatisfactory, even in curatively resected patients where the 5-year survival rate is <50% after surgery.[3] Several prognostic markers, such as nodal status and tumor stage, are currently accepted for clinical use, and we have previously reported several ESCC-associated genes.[4–7] However, these genes cannot completely identify which patients are at low or high risk for disease recurrence. Therefore, identification of novel prognostic markers for patients with ESCC is important.

Expression of the *KRT7* gene, which encodes cytokeratin 7 (CK7), has been identified by microarray analysis to be involved in the poor prognosis of ESCC patients.[8] CK7 is expressed in several simple ductal epithelia, in mesothelium, and in urothelium. However, CK7 is sparsely

expressed or absent in gastric foveolar epithelium, intestinal epithelium, hepatocytes, and squamous epithelia.[9] A direct association between CK7 expression and poor prognosis of ESCC patients remains unclear. It has been suggested that because CK7 expression is regulated by the forkhead box A1 (FOXA1) transcription factor, FOXA1 may also regulate several cancer-related genes, such as *LOXL2,* in CK7-positive ESCC cases.[8] It has been also reported that CK7 expression is a statistically significant prognostic factor in patients with stage I and II ESCC.[10] However, the impact of immunohistochemically detected CK7 expression on prognosis or therapeutic outcome in patients with stage I–III ESCC remains unclear.

In the present study, immunohistochemical analysis of CK7 was performed in a large number of primary ESCC samples ($n = 225$). In addition, associations between CK7 expression and therapeutic outcomes in stage II and III ESCC patients were investigated.

MATERIALS AND METHODS

Tissue Samples

In a retrospective study design, 225 primary tumors were collected from patients diagnosed with ESCC who underwent surgery between 1990 and 2002 at Hiroshima University Hospital (Hiroshima, Japan). All patients underwent curative resection. All patients underwent right transthoracic esophagectomy with extensive lymph node dissection. Reconstruction was performed with a gastric tube positioned in the posterior mediastinum. Only patients without preoperative radiotherapy or chemotherapy and without clinical evidence of distant metastasis were enrolled in the study. Operative mortality was defined as death within 30 days of patients leaving the hospital, and these patients removed from the analysis. Characteristics of the study population are shown in the Supplementary Table 1. The disease-free survival (DFS) median follow-up time was 25 months (range 1–80 months) and the overall survival (OS) median follow-up time was 27 months (range 1–80 months). Postoperative follow-up was scheduled every 1, 2, or 3 months during the first 2 years after surgery and every 6 months thereafter unless more frequent follow-up was deemed necessary. Chest X-ray, chest computed tomographic scan, and serum chemistries were performed at every follow-up visit. Patients were followed by the patients' physician until their death or the date of the last documented contact.

For immunohistochemical analysis, we used archival formalin-fixed, paraffin-embedded tissues. Histologic classification was based on the World Health Organization system. Tumor staging was performed according to the tumor, node, metastasis system stage grouping system.[11] As a retrospective study where written informed consent was not obtained, identifying information for all samples was removed before analysis for strict privacy protection. These procedures were in accordance with the ethical guidelines for human genome/gene research enacted by the Japanese government. This study was approved by the Ethical Committee for Human Genome Research of Hiroshima University (Hiroshima, Japan).

Immunohistochemistry

One or two representative tumor blocks, including the tumor center, invading front, and tumor-associated non-neoplastic mucosa, was examined from each patient by immunohistochemistry. In cases of large, late-stage tumors, two different sections were examined to include representative areas of the tumor center as well as of the lateral and deep tumor invasive front. Immunohistochemical analysis was performed with a Dako Envision+ Mouse Peroxidase Detection System (Dako Cytomation, Carpinteria, CA). Antigen retrieval was performed by microwave heating in citrate buffer (pH 6.0) for 30 min. Peroxidase activity was blocked with 3% H_2O_2–methanol for 10 min, and sections were incubated with normal goat serum (Dako Cytomation) for 20 min to block nonspecific antibody binding sites. Sections were incubated with a mouse monoclonal anti-CK7 antibody (1:50, Clone OV-TL 12/30, Dako Cytomation) for 1 hour at room temperature, followed by incubation with Envision+ anti-mouse peroxidase for 1 hour. For color reaction, sections were incubated with the DAB substrate–chromogen solution (Dako Cytomation) for 10 min. Sections were counterstained with 0.1% hematoxylin. Negative controls were created by omission of the primary antibody.

Expression of CK7 was scored in all tumors as positive or negative. When more than 10% of tumor cells were stained, the immunostaining was considered positive for CK7. By using these definitions, two surgical pathologists (N.O. and K.S.), without knowledge of the clinical and pathologic parameters or the patients' outcomes, independently reviewed immunoreactivity in each specimen. Interobserver differences were resolved by consensus review at a double-headed microscope after independent review.

Statistical Methods

Correlations between clinicopathologic parameters and CK7 expression were analyzed by the chi-square test. Kaplan–Meier survival curves were constructed for CK7-positive and CK7-negative patients. Survival rates were compared between CK7-positive and CK7-negative groups. Differences between survival curves of DFS and OS were tested for statistical significance by the log rank

test. Univariate and multivariate Cox regression was used to evaluate the associations between clinical covariates and DFS or OS. SPSS software was used for these analyses (SPSS, Chicago, IL). Hazard ratio (HR) and 95% confidence interval (CI) were estimated from Cox proportional hazard models. For all analyses, age was treated as a categorical variable (65 years or more vs. less than 65 years). For final multivariable Cox regression models, all variables were included that were moderately associated ($P < 0.10$) with DFS or OS by univariate analysis. A P value of less than 0.05 was considered statistically significant.

RESULTS

Immunohistochemical Analysis of CK7 in ESCC

CK7 staining was detected in 55 (24%) of the 225 ESCC specimens investigated. In the nonneoplastic esophageal mucosa adjacent to the tumor, no CK7 staining was observed in squamous epithelial and stromal cells. As reported previously, the esophageal gland was stained by CK7 (Fig. 1a)[12]. Of the 55 ESCC cases in which CK7 staining was detected, 35 cases showed only weak staining of the cytoplasm of tumor cells. In 20 ESCC cases, strong staining was observed in the cytoplasm of tumor cells (Fig. 1b). Expression of CK7 was observed in some cases of squamous cell carcinoma-in-situ (Fig. 1c). When more than 10% of tumor cells were stained, the immunostaining was considered positive for CK7. In total, 20 (9%) of 225 ESCC cases were positive for CK7. We analyzed the relationship between CK7 expression and clinicopathologic characteristics. CK7-positive ESCC cases were more advanced in terms of T classification ($P = 0.0014$, χ^2 test), N classification ($P = 0.0195$, χ^2 test), and tumor stage ($P = 0.0016$, χ^2 test) than CK7-negative ESCC cases (Table 1). Expression of CK7 was not associated with age, sex, or histologic classification.

Relationship Between CK7 Staining and Prognosis of Patients with Stage 0–III ESCC

The association between CK7 expression and DFS or OS was investigated by Kaplan–Meier analysis in all ESCC samples (stage 0–III, $n = 225$). We found that CK7 expression was significantly associated with both poorer DFS and OS ($P = 0.0044$ and $P = 0.0075$, log rank test, respectively; Fig. 2a). Univariate and multivariate Cox proportional hazards analysis was used to further evaluate the association between CK7 expression and DFS (Supplementary Table 2) or OS (Supplementary Table 3). The univariate analysis indicated that expression of CK7 (HR 2.72; 95% CI 1.32–5.59; $P = 0.0066$), tumor stage (HR 13.89; 95% CI 5.03–38.46; $P < 0.0001$), and adjuvant chemotherapy (HR 1.88; 95% CI 1.07–3.32; $P = 0.0293$) were associated with DFS while age, sex, or histologic classification were not. We next performed multivariate model, which included CK7 expression, tumor stage, and adjuvant chemotherapy. However, CK7 expression was not an independent prognostic indicator of DFS (HR 2.01; 95% CI 0.97–4.17; $P = 0.0616$). The univariate analysis

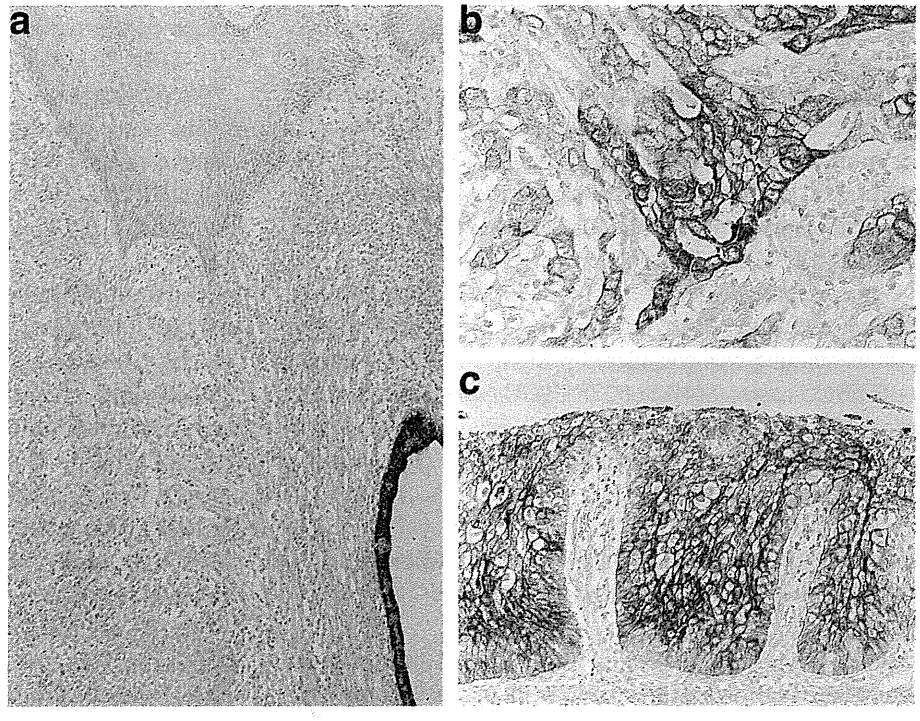

FIG. 1 Immunohistochemical analysis of CK7 in ESCC tissues. In the nonneoplastic esophageal mucosa adjacent to the tumor, esophageal glands were stained by CK7, but squamous epithelium was negative (**a**) (original magnification, 100×). Strong and extensive staining was observed in the cytoplasm of ESCC cells (**b**) (original magnification, 400×). Expression of CK7 was observed in some cases of squamous cell carcinoma-in-situ (**c**) (original magnification, 200×)

TABLE 1 Relationship between cytokeratin 7 (CK7) expression and clinicopathologic characteristics in esophageal squamous cell carcinoma

Characteristic	CK7 expression		
	Positive (%)	Negative	P^a
Age			
<66 years	8 (7)	104	0.4832
≥66 years	12 (11)	101	
Sex			
Male	17 (9)	178	0.7360
Female	3 (10)	27	
T classification			
Tis/1	6 (5)	121	0.0014
T2	1 (5)	21	
T3	12 (16)	62	
T4	1 (50)	1	
N classification			
N0	6 (30)	14	0.0195
N1	120 (59)	85	
Tumor stage			
0/I	4 (4)	97	0.0016
II	5 (8)	60	
III	11 (19)	48	
Histologic classification			
Well/moderate	16 (10)	151	0.7890
Poor	4 (7)	54	

[a] χ^2 test

indicated that expression of CK7 (HR 2.70; 95% CI 1.26–5.78; $P = 0.0110$) and tumor stage (HR 17.24; 95% CI 5.32–55.56; $P < 0.0001$) were associated with OS, while age, sex, and histologic classification were not. Adjuvant chemotherapy was moderately associated with OS (HR 1.81; 95% CI 0.99–3.33; $P = 0.0562$). We also performed multivariate model, which included CK7 expression, tumor stage, and adjuvant chemotherapy. CK7 expression was an independent prognostic indicator of OS (HR 2.24; 95% CI 1.03–4.88; $P = 0.0426$).

We performed survival analysis with other cutoff point. When more than 25% of tumor cells were stained, the immunostaining was considered positive for CK7. In stage 0–III ESCC cases, 9 (4%) of 225 ESCC cases were positive for CK7, and similar results were obtained (data not shown). These results demonstrate that CK7 expression is a useful predictor of OS.

Relationship Between CK7 Staining and Prognosis of Patients with Stage II and III ESCC

Patients with ESCC at stage 0 and stage I have a good rate of survival, whereas patients with ESCC at stage IV show a poor rate of survival. However, it is difficult to predict the survival of patients with stage II or stage III ESCC, and these patients would benefit the most from prognostic biomarkers. Therefore, we analyzed the prognostic value of CK7 expression in patients with stage II and III ESCC ($n = 124$). In Kaplan–Meier analysis, we found that CK7 expression was significantly associated with both poorer DFS and OS (respectively, $P = 0.0472$ and $P = 0.0377$, log rank test; Fig. 2b). Because adjuvant chemotherapy for patients with stage II and stage III ESCC influences survival, we analyzed individuals who did not receive adjuvant chemotherapy ($n = 73$). We found that CK7 expression was significantly associated with both poorer DFS and OS in stage II and III ESCC patients who did not receive adjuvant chemotherapy (respectively, $P = 0.0008$ and $P = 0.0003$, log rank test; Fig. 3a).

To evaluate the potential for CK7 expression as a prognostic predictor in patients with stage II and III ESCC, both univariate and multivariate Cox proportional hazards analyses were used to further evaluate the association of CK7 expression with DFS (Table 2) or OS (Table 3). In univariate analysis, CK7 expression (HR 2.05; 95% CI 0.99–4.27; $P = 0.0548$) was moderately associated with DFS. We next performed multivariate model, which included CK7 expression and the tumor stage. However, CK7 expression was not an independent prognostic classifier of DFS (HR 1.77; 95% CI 0.85–3.70; $P = 0.1297$). In univariate analysis, CK7 expression (HR 2.22; 95% CI 1.02–4.83; $P = 0.0450$) and tumor stage (HR 2.97; 95% CI 1.57–5.62; $P = 0.0008$) were associated with OS. We also performed multivariate model, which included CK7 expression and the tumor stage. CK7 expression was an independent prognostic predictor of OS (HR 2.25; 95% CI 1.01–5.00; $P = 0.0474$).

We performed survival analysis with other cutoff point. When more than 25% of tumor cells were stained, the immunostaining was considered positive for CK7. In stage II and III ESCC cases, 7 (6%) of 124 cases were positive for CK7, and similar results were obtained (data not shown).

Because CK7 staining was detected in ESCC in situ, we analyzed the prognostic value of CK7 expression in patients with stage 0 and stage I ESCC ($n = 101$). When more than 10% of tumor cells were stained, the immunostaining was considered positive for CK7. In total, 4 (4%) of 101 cases were positive for CK7. CK7 expression was not associated with DFS or OS in Kaplan–Meier analysis (data not shown). We also performed survival analysis with another cutoff point. When more than 25% of tumor cells were stained, the immunostaining was considered positive for CK7. In total, 2 (2%) of 101 ESCC cases were positive for CK7. However, CK7 expression was not associated with DFS or OS in Kaplan–Meier analysis (data not shown).

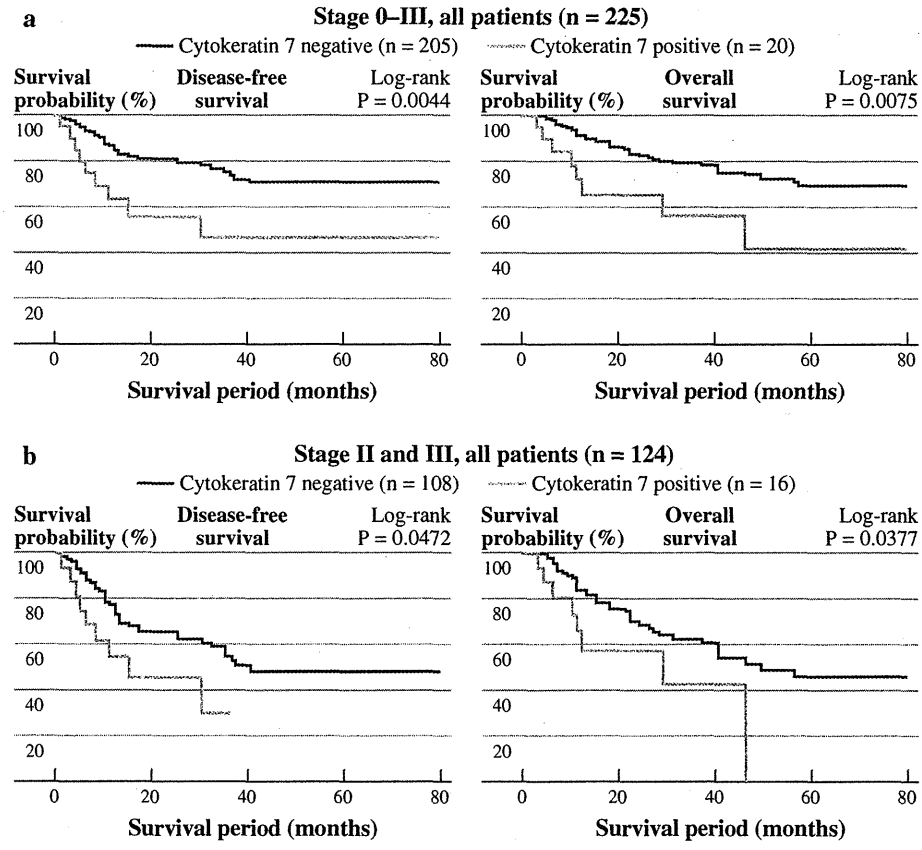

FIG. 2 Disease-free survival and overall survival of patients with ESCC. Kaplan–Meier curves of **a** CK7-positive or CK7-negative ESCC in stage 0–III patients and of **b** patients with stage II and III disease

These results indicate that CK7 expression is associated with OS but not DFS in patients with stage II and III ESCC.

CK7 Expression and Therapeutic Outcome

Biomarkers that can predict therapeutic outcomes may provide tools to allow physicians to better stratify patients to more effective treatments. We analyzed associations between CK7 expression and therapeutic outcomes in stage II and III ESCC patients. Information regarding the administration of adjuvant chemotherapy was available for all patients. Chemotherapy regimens were primarily 5-fluorouracil based. In stage II and III ESCC patients who received adjuvant chemotherapy ($n = 51$), adjuvant chemotherapy was not found to be beneficial. Furthermore, CK7 expression was not significantly associated with therapeutic outcome in patients with stage II and III ESCC (Fig. 3b). These results indicate that CK7 expression cannot predict therapeutic outcome in patients with stage II and III ESCC.

Although we performed survival analysis with another cutoff point, CK7-positive cases were not found in patients who received adjuvant chemotherapy when the cutoff value was set at 25%. Therefore, we set cutoff value at 10% in the following analysis.

Efficacy of Adjuvant Chemotherapy in CK7-Positive and CK7-Negative Patients

We have demonstrated that CK7 expression has the potential to identify patients at high risk of cancer-specific mortality. Furthermore, our data have demonstrated that CK7-positive cases had significantly worse cancer-specific mortality than CK7-negative cases in stage II and III ESCC patients who did not receive adjuvant chemotherapy. These results indicate that CK7 expression is associated with a more aggressive histology of the primary tumor. Because CK7-positive ESCC cases had significantly worse cancer-specific mortality than CK7-negative ESCC cases, adjuvant chemotherapy may be indicated for patients with CK7-positive ESCC. However, it is unclear whether such patients may benefit from adjuvant chemotherapy. To address this issue, we examined whether CK7 expression can identify patients for whom adjuvant chemotherapy is beneficial in stage II and III ESCC. Although in patients with CK7-positive ESCC ($n = 16$) there is a trend toward improved survival with the use of adjuvant chemotherapy in CK7-positive ESCC, therapeutic outcome between patients with CK7-positive and CK7-negative ESCC was not significantly different (Fig. 3c). Conversely, CK7-negative patients with ESCC ($n = 108$) did not benefit

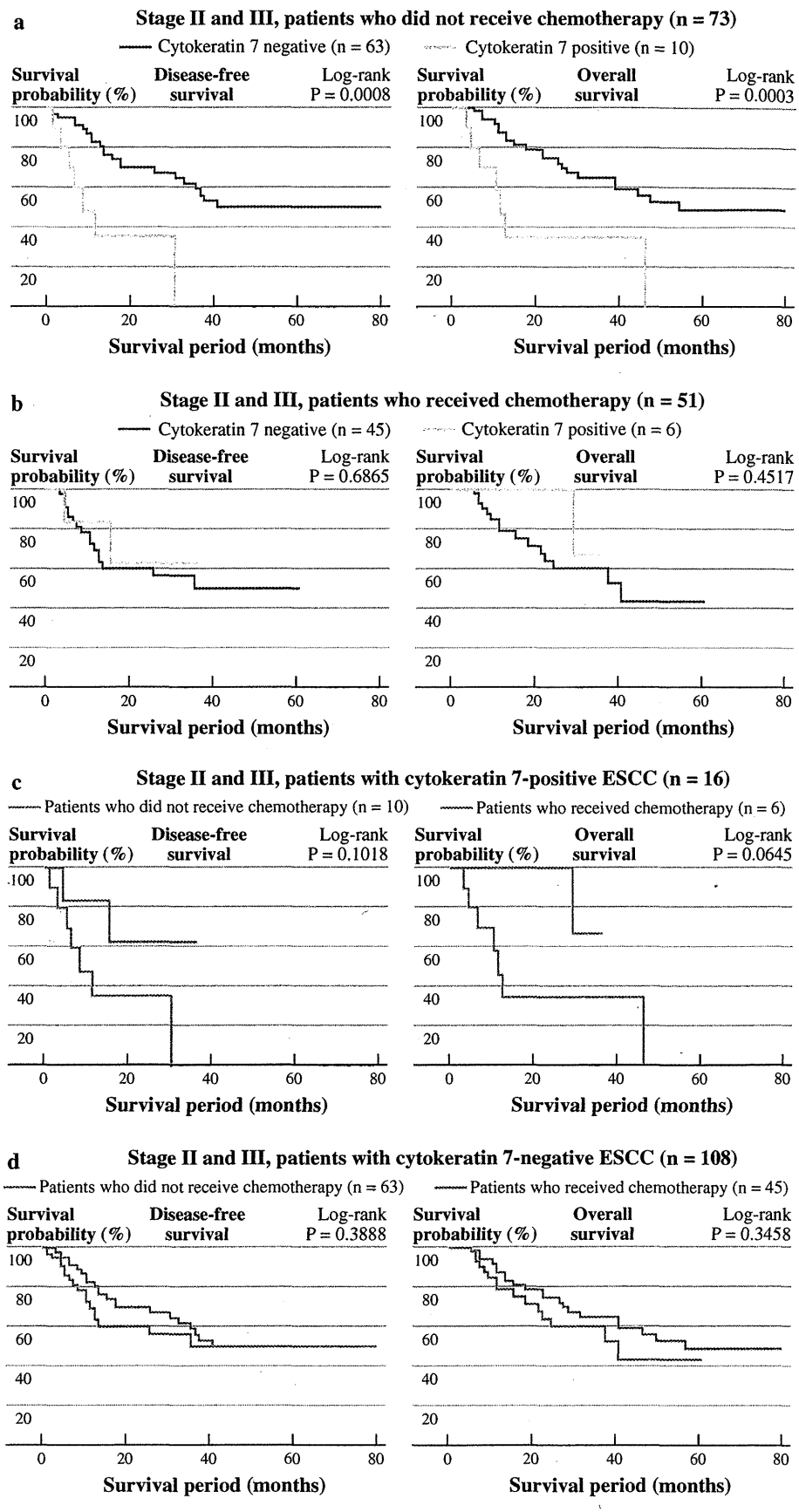

FIG. 3 Disease-free survival and overall survival of patients with stage II and III ESCC. Kaplan–Meier curves of CK7-positive or CK7-negative ESCC in stage II and III ESCC patients who did not receive adjuvant chemotherapy (**a**); stage II and III patients who received adjuvant chemotherapy (**b**); stage II and III CK7-positive ESCC patients with or without adjuvant chemotherapy (**c**); stage II and III CK7-negative ESCC patients with or without adjuvant chemotherapy (**d**)

TABLE 2 Univariate and multivariate Cox regression analysis of CK7 expression and disease-free survival in esophageal squamous cell carcinoma (stage II and III, $n = 124$)

Characteristic	MST, mo	Univariate analysis		Multivariate analysis	
		HR (95% CI)	*P*	HR (95% CI)	*P*
CK7 expression					
Negative	40	1 (Ref.)	0.0548	1 (Ref.)	0.1297
Positive	15	2.05 (0.99–4.27)		1.77 (0.85–3.70)	
Tumor stage					
II	NR	1 (Ref.)	0.0018	1 (Ref.)	0.0032
III	15	2.57 (1.42–4.65)		2.46 (1.35–4.46)	
Adjuvant chemotherapy					
Not received	NR	1 (Ref.)	0.8933		
Received	36	1.04 (0.58–1.86)			
Age					
≥66 years	NR	1 (Ref.)	0.5596		
<66 years	32	1.19 (0.67–2.10)			
Sex					
Female	NR	1 (Ref.)	0.1324		
Male	35	2.46 (0.76–7.94)			
Histologic classification					
Well/moderate	NR	1 (Ref.)	0.3023		
Poor	32	1.37 (0.75–2.50)			

CK7 Cytokeratin 7, *HR* hazard ratio, *CI* confidence interval, *NR* not reached, *MST* median survival time

TABLE 3 Univariate and multivariate Cox regression analysis of CK7 expression and overall survival in esophageal squamous cell carcinoma (stage II and III, $n = 124$)

Characteristic	MST, mo	Univariate analysis		Multivariate analysis	
		HR (95% CI)	*P*	HR (95% CI)	*P*
CK7 expression					
Negative	49	1 (Ref.)	0.0450	1 (Ref.)	0.0474
Positive	29	2.22 (1.02–4.83)		2.25 (1.01–5.00)	
Tumor stage					
II	NR	1 (Ref.)	0.0008	1 (Ref.)	0.0018
III	46	2.97 (1.57–5.62)		2.98 (1.50–5.92)	
Adjuvant chemotherapy					
Not received	46	1 (Ref.)	0.9433		
Received	40	1.02 (0.55–1.91)			
Age					
≥66 years	NR	1 (Ref.)	0.6711		
<66 years	46	1.19 (0.65–2.17)			
Sex					
Female	NR	1 (Ref.)	0.2134		
Male	46	2.11 (0.65–6.80)			
Histologic classification					
Well/moderate	49	1 (Ref.)	0.2689		
Poor	37	1.41 (0.76–2.62)			

CK7 Cytokeratin 7, *HR* hazard ratio, *CI* confidence interval, *NR* not reached, *MST* median survival time

from adjuvant chemotherapy (Fig. 3d). These results demonstrate the potential for the use of CK7 immunohistochemistry to identify patients who can benefit from adjuvant chemotherapy.

DISCUSSION

The long-term survival of patients with ESCC remains poor as a result of the high incidence of lymph node metastasis and early recurrence after curative surgical resection. In the present study, we performed immunohistochemical analysis of CK7 in 225 ESCC cases. Univariate and multivariate analyses revealed that CK7 expression is an independent prognostic classifier of OS in stage 0–III ESCC. We previously reported that patients with CK7-positive ESCC have a worse prognosis for stage I and II ESCC in a cohort from the National Cancer Center Hospital East (Kashiwa, Japan).[10] Therefore, the usefulness of CK7 immunohistochemical analysis is now shown in two independent cohorts. Taken together, these results indicate that immunohistochemical analysis of CK7 is a clinically useful method for prediction of survival of patients with ESCC.

Patients diagnosed with stage II or stage III ESCC have variable prognoses. These groups would benefit from the discovery of prognostic markers that identify individuals for whom adjuvant treatment would be advantageous. In the present study, we demonstrated that CK7 expression was associated with the OS of patients with stage II and stage III ESCC. This indicates that immunohistochemical analysis of CK7 may help identify patients with a high risk of disease recurrence. In the present study, CK7 expression was associated with DFS and OS in stage II and III ESCC patients who did not receive adjuvant chemotherapy. In contrast, CK7 expression was not associated with therapeutic outcome in patients with stage II and III ESCC who received adjuvant chemotherapy. These results suggest that adjuvant chemotherapy may improve survival of patients with CK7-positive ESCC. Although there is a trend toward improved survival with the use of adjuvant chemotherapy in CK7-positive ESCC, therapeutic outcome between patients with CK7-positive and CK7-negative ESCC was not significantly different. As the number of CK7-positive stage II and III ESCC cases was small ($n = 16$), this result should be further investigated in a large ESCC cohort.

The mechanisms underlying the associations between CK7 expression and patients' survival remains unclear. It has been suggested that CK7 expression may be regulated by the FOXA1 transcription factor because *KRT7* mRNA expression levels correlate with *FOXA1* mRNA expression levels.[8] In the TE3 esophageal cancer cell line, knockdown of FOXA1 by siRNA inhibits cell migration and CK7 expression.[8] Therefore, CK7 may be a marker for ESCC expressing FOXA1, and some genes induced by FOXA1 may be associated with cell migration. In addition to CK7, immunohistochemical analysis of FOXA1 may also have the potential to predict patient survival. In the present study, there is a trend toward improved survival with the use of adjuvant chemotherapy in CK7-positive ESCC. To our knowledge, a direct association between CK7 and chemotherapy efficacy has not been investigated. It is possible that some genes induced by FOXA1 may enhance the efficacy of adjuvant chemotherapy in ESCC.

In summary, we have shown that CK7 expression is an independent prognostic classifier in patients with ESCC. Furthermore, there is a trend toward improved survival with the use of adjuvant chemotherapy in CK7-positive ESCC. It is possible that immunohistochemical analysis of CK7 may help identify patients who would benefit from adjuvant chemotherapy. Identification of FOXA1 target genes may improve our understanding of the characteristics of CK7-positive ESCC.

ACKNOWLEDGMENT We thank Shinichi Norimura for his technical assistance and advice. This work was carried out with the cooperation of the Research Center for Molecular Medicine of the Faculty of Medicine of Hiroshima University. We thank the Analysis Center of Life Science of Hiroshima University for the use of their facilities. This work was supported in part by grants-in-aid for Cancer Research from the Ministry of Education, Culture, Science, Sports and Technology of Japan and in part by a grant-in-aid for the Third Comprehensive 10-Year Strategy for Cancer Control from the Ministry of Health, Labor and Welfare of Japan, and by the National Institute of Biomedical Innovation (Program for Promotion of Fundamental Studies in Health Sciences) and by National Cancer Center Research and Development Fund.

REFERENCES

1. IARC 2003 Oesophageal cancer. In: Stewart BW, Kleihues P (eds) World cancer report. Lyon: IARC Press, pp. 223–7.
2. Goseki N, Koike M, Yoshida M. Histopathologic characteristics of early stage esophageal carcinoma. A comparative study with gastric carcinoma. *Cancer.* 1992;69:1088–93.
3. Courrech Staal EF, van Coevorden F, Cats A, Aleman BM, van Velthuysen ML, Boot H et al. Outcome of low-volume surgery for esophageal cancer in a high-volume referral center. *Ann Surg Oncol.* 2009;16:3219–26.
4. Takeno S, Noguchi T, Kikuchi R, Uchida Y, Yokoyama S, Müller W. Prognostic value of cyclin B1 in patients with esophageal squamous cell carcinoma. *Cancer.* 2002;94:2874–81.
5. Noguchi T, Oue N, Wada S, Sentani K, Sakamoto N, Kikuchi A et al. h-Prune is an independent prognostic marker for survival in esophageal squamous cell carcinoma. *Ann Surg Oncol.* 2009;16:1390–6.
6. Isohata N, Aoyagi K, Mabuchi T, Daiko H, Fukaya M, Ohta H et al. Hedgehog and epithelial-mesenchymal transition signaling in normal and malignant epithelial cells of the esophagus. *Int J Cancer.* 2009;125:1212–21.
7. Sakamoto N, Oue N, Noguchi T, Sentani, K., Anami, K., Sanada, Y, et al. Serial analysis of gene expression of esophageal

squamous cell carcinoma: ADAMTS16 is upregulated in esophageal squamous cell carcinoma. *Cancer Sci.* 2010;101:1038–44.
8. Sano M, Aoyagi K, Takahashi H, Kawamura T, Mabuchi T, Igaki H, et al. Forkhead box A1 transcriptional pathway in KRT7-expressing esophageal squamous cell carcinomas with extensive lymph node metastasis. *Int J Oncol.* 2010;36:321–30.
9. Moll R, Divo M, Langbein L. The human keratins: biology and pathology. *Histochem Cell Biol.* 2008;129:705–33.
10. Yamada A, Sasaki H, Aoyagi K, Sano M, Fujii S, Daiko H, et al. Expression of cytokeratin 7 predicts survival in stage I/IIA/IIB squamous cell carcinoma of the esophagus. *Oncol Rep.* 2008;20:1021–7.
11. Sobin LH, Wittekind CH, editors. TNM classification of malignant tumors. 6th ed. New York: Wiley-Liss, 2002:60–4.
12. Haleem A, Kfoury H, Al Juboury M, Al Husseini H. Paget's disease of the oesophagus associated with mucous gland carcinoma of the lower oesophagus. *Histopathology.* 2003;42:61–5.

OPEN ACCESS Freely available online

PLOS | ONE

Reg IV Is a Direct Target of Intestinal Transcriptional Factor CDX2 in Gastric Cancer

Yutaka Naito[1], Naohide Oue[1], Takao Hinoi[2], Naoya Sakamoto[1], Kazuhiro Sentani[1], Hideki Ohdan[2], Kazuyoshi Yanagihara[3], Hiroki Sasaki[3], Wataru Yasui[1]*

1 Department of Molecular Pathology, Hiroshima University Graduate School of Biomedical Sciences, Hiroshima, Japan, **2** Department of Surgery, Hiroshima University Graduate School of Biomedical Sciences, Hiroshima, Japan, **3** Division of Genetics, National Cancer Center Research Institute, Tokyo, Japan

Abstract

REG4, which encodes Reg IV protein, is a member of the calcium-dependent lectin superfamily and potent activator of the epidermal growth factor receptor/Akt/activator protein-1 signaling pathway. Several human cancers overexpress Reg IV, and Reg IV expression is associated with intestinal phenotype differentiation. However, regulation of *REG4* transcription remains unclear. In the present study, we investigated whether CDX2 regulates Reg IV expression in gastric cancer (GC) cells. Expression of Reg IV and CDX2 was analyzed by Western blot and quantitative reverse transcription–polymerase chain reaction in 9 GC cell lines and 2 colon cancer cell lines. The function of the 5′-flanking region of the *REG4* gene was characterized by luciferase assay. In 9 GC cell lines, endogenous Reg IV and CDX2 expression were well correlated. Using an estrogen receptor-regulated form of CDX2, rapid induction of Reg IV expression was observed in HT-29 cells. Reporter gene assays revealed an important role in transcription for consensus CDX2 DNA binding elements in the 5′-flanking region of the *REG4* gene. Chromatin immunoprecipitation assays showed that CDX2 binds directly to the 5′-flanking region of *REG4*. These results indicate that CDX2 protein directly regulates Reg IV expression.

Citation: Naito Y, Oue N, Hinoi T, Sakamoto N, Sentani K, et al. (2012) Reg IV Is a Direct Target of Intestinal Transcriptional Factor CDX2 in Gastric Cancer. PLoS ONE 7(11): e47545. doi:10.1371/journal.pone.0047545

Editor: Wael El-Rifai, Vanderbilt University Medical Center, United States of America

Received May 24, 2012; **Accepted** September 12, 2012; **Published** November 2, 2012

Funding: This work was supported by Grants-in-Aid for Research from the Ministry of Education, Culture, Science, Sports, and Technology of Japan, and, in part, by a Grant-in-Aid for the Third Comprehensive 10-Year Strategy for Cancer Control and for Cancer Research from the Ministry of Health, Labour and Welfare of Japan, and for the National Institute of Biomedical Innovation (Program for Promotion of Fundamental Studies in Health Sciences). The funders had no role in study design, data collection and analysis, decision to publish, or preparation of the manuscript.

Competing Interests: The authors have declared that no competing interests exist.

* E-mail: wyasui@hiroshima-u.ac.jp

Introduction

Gastric cancer (GC) is one of the most common human cancers in the world. Cancer develops as a result of multiple genetic and epigenetic alterations [1]. We previously performed serial analysis of gene expression (SAGE) of four primary GCs and identified several GC-specific genes [2]. Of these genes, *regenerating islet-derived family member 4* (*REG4*, which encodes Reg IV protein) is a candidate gene for cancer-specific expression [3]. *REG4* is a member of the *REG* gene family, which belongs to the calcium-dependent lectin superfamily. *REG4* was originally identified by high-throughput sequence analysis of a large inflammatory bowel disease cDNA library [4]. Reg IV is a potent activator of the epidermal growth factor receptor (EGFR)/Akt/activator protein-1 (AP-1) signaling pathway in colon cancer cells and increases expression of Bcl-2, Bcl-xl and survivin, which are proteins associated with the inhibition of apoptosis [5]. Amplification of the *REG4* gene has been reported in pancreatic cancer [6]. Reg IV has been identified as one of the genes up-regulated in cancer-initiating cells [7]. We have previously examined the effect of forced expression of Reg IV in GC cell line. We showed that Reg IV inhibits 5-fluorouracil (5-FU)-induced apoptosis through EGFR activation in GC cells [8]. In contrast, Reg IV-overexpressing cells did not show significant differences in proliferation and invasion activity compared with cells transfected with empty vector [8]. These findings support the notion that Reg IV protein participates in gastric carcinogenesis.

GC can be subdivided into four phenotypes according to mucin expression: gastric or foveolar phenotype; intestinal phenotype; intestinal and gastric mixed phenotype; and neither gastric nor intestinal phenotype [9]. Distinct genetic changes appear to be associated with gastric and intestinal phenotype GC [10]. In our previous observations, Reg IV was expressed in 30% of GC cases and was correlated with intestinal phenotype [11]. A number of immunohistochemical analyses of Reg IV have been reported in human cancers [11–20]. In general, these analyses reported that Reg IV is expressed in adenocarcinoma cells displaying an intestinal phenotype. It has been reported that Reg IV expression is induced by GLI1, which is a key transcriptional factor in the Hedgehog signaling pathway [21], or by growth factors such as EGF, transforming growth factor-α (TGF-α), hepatocyte growth factor (HGF), or basic fibroblast growth factor (bFGF) [22]. However, these molecules are unlikely to account for the association between Reg IV expression and intestinal phenotype differentiation.

We have previously found that expression of Reg IV was correlated with CDX2 expression [11]. CDX2 is a mammalian caudal-related intestinal transcription factor and important for the maintenance of intestinal epithelial cells [23,24]. Several lines of evidence suggest that intestinal metaplasia of the stomach and

intestinal phenotype GC are associated with ectopic CDX2 expression [9,25]. In the present study, we investigated whether CDX2 regulates Reg IV expression in GC and found that CDX2 directly binds to the 5′-flanking region of *REG4* gene and enhances the promoter activity.

Results

Reg IV and CDX2 Expression are Correlated in GC Cells

We first investigated induction of Reg IV expression by CDX2 in GC cell lines. Western blot analysis of CDX2 in 9 GC cell lines revealed that no or low-level expression of CDX2 was detected in MKN-7, TMK-1, HSC-44PE, and KATO-III (**Fig. 1A**). To determine if CDX2 and Reg IV expression were tightly correlated in GC cells, Western blot and quantitative reverse transcription–polymerase chain reaction (qRT-PCR) analyses of Reg IV were performed on 9 GC cell lines. As shown in **Fig. 1A**, Reg IV protein expression was only detected in the 3 cell lines with high levels of *REG4* transcripts measured by qRT-PCR. Of the 5 GC cell lines with CDX2 protein expression, 2 cell lines (MKN-1 and MKN-28) lacked detectable expression of *REG4* transcripts and protein. The cell lines with undetectable CDX2 protein expression (MKN-7, TMK-1, HSC-44PE, and KATO-III) did not show *REG4* transcripts or protein (**Fig. 1A**).

Next, we generated a polyclonal population of MKN-7, TMK-1, HSC-44PE, and KATO-III cells expressing high levels of CDX2 by infection of the cells with replication-defective retroviruses carrying a full-length human CDX2 cDNA because no or low-level expression of CDX2 was detected in these cell lines. However, overexpression of CDX2 failed to activate Reg IV expression by Western blot (**data not shown**). Because it is possible that CDX2 alone is not sufficient for activating Reg IV expression, expression of *CDH17* (encoding LI-cadherin protein), which is one of the targets of CDX2 [24], was also investigated. However, activation of LI-cadherin expression was not found in MKN-7, TMK-1, HSC-44PE, and KATO-III cells expressing high levels of CDX2 (**data not shown**). Because we showed activation of LI-cadherin expression by CDX2 in the HT-29 colon cancer cell line [24], induction of Reg IV expression was investigated in the same cell line. As shown in **Fig. 1B**, induction of Reg IV expression was detected in HT-29 cells infected with retroviruses carrying a full-length human CDX2 cDNA. We also generated a polyclonal population of SW480 (colon cancer cell line) cells expressing high levels of CDX2 by infection of the cells with replication-defective retroviruses carrying a full-length human CDX2 cDNA. As shown in **Fig. 1B**, induction of Reg IV expression was found in SW480 cells infected with retroviruses carrying a full-length human CDX2 cDNA. These results suggest that Reg IV expression can be induced by CDX2 in cell lines derived from colon cancer. Because in intestinal metaplasia of the stomach, CDX2 and Reg IV expression are well correlated [11], the use of a colon cancer cell line might be suitable for the model of intestinal metaplasia.

To better assess the relationship between CDX2 and Reg IV expression, we studied Reg IV expression in an HT-29-derived line with tightly regulated CDX2 activity. We used a polyclonal HT-29 cell line that had been transduced with the pCDX2-ER vector. The pCDX2-ER vector encodes a chimeric protein in which full-length CDX2 sequences are fused upstream of a mutated estrogen receptor (ER) ligand–binding domain. The mutated ER ligand-binding domain no longer binds estrogen, but retains the ability to bind tamoxifen. Treatment of the HT-29/CDX2-ER cell line with 4-hydroxytamoxifen (4-OHT) resulted in strong induction of Reg IV protein expression within 48 hours (**Fig. 1C**). These results indicate that Reg IV is a direct or primary target gene regulated by CDX2. However, CDX2 alone is not sufficient for activating Reg IV expression.

Inhibition of CDX2 by RNA Interference (RNAi) Results in the Down-regulation of Reg IV in GC Cells

To determine whether CDX2 is necessary for Reg IV expression in GC cells, we analyzed the effect of inhibiting CDX2 expression by RNAi in the level of Reg IV expression in HSC-39 cell line because high endogenous CDX2 and Reg IV expression was detected in HSC-39 cell line. CDX2-specific small interfering RNAs (siRNAs) significantly suppressed CDX2 protein expression 3 days after transfection, and expression of Reg IV transcript was down-regulated approximately 50% by CDX2 siRNAs in HSC-39 compared with its levels in control siRNA-treated cells (**Fig. 1D**). These results indicate that CDX2 is involved in maintaining Reg IV gene expression.

Functional Characterization the 5′-flanking Region of *REG4* Gene by Luciferase Assay

To identify potential CDX2-binding sites in the *REG4* promoter region, a search of the genomic sequences immediately 5′ to the presumptive transcription start site was performed, using a consensus binding element for the CdxA chicken *caudal* homologue (5′-A, A/T, T, A/T, A, T, A/G-3′) [26] and a previously described search algorithm [27]. We found four putative CDX2-binding sites in the 2 kilobase (kb) 5′-flanking region of the *REG4* gene (**Fig. 2A**). These were: site A (5′-AATAATA-3′, from −1828 to −1834), site B (5′-CTTTACAG-3′, from −901 to −908), site C (5′-TTTTATGG-3′, from −114 to −121), site D (5′-AATAATA -3′, from −90 to −96). To assess the role of these presumptive CDX2-binding sites in regulating *REG4* transcription, various reporter gene constructs were generated. As shown in **Fig. 2B**, reporter gene constructs containing 2.1, 1.2, or 0.6 kb of 5′-flanking sequence from the *REG4* gene showed strong activity in the HSC-39 cells, which display strong endogenous expression of *REG4* transcripts and protein. By comparison, MKN-1 cells have little endogenous *REG4* transcript and displayed little or no transcriptional activity induced by the 2.1, 1.2, or 0.6 kb *REG4* reporter gene constructs (**data not shown**). The *REG4* reporter gene constructs containing base pairs −116 to +58 and −87 to +58 had reduced activity in the HSC-39 cells (**Fig. 2B**), indicating that sequences between base pairs −634 and −116 play a key role in activating *REG4* transcription. Furthermore, we analyzed single and multiple mutations in the presumptive CDX2-binding sites in the 5′-flanking region of the *REG4* gene using HSC-39 cells (**Fig. 2C**). As expected, presumptive CDX2-binding site C, which is located between base pairs −634 and −116, plays a crucial role in activating *REG4* transcription.

CDX2 Directly Binds to the 5′-flanking Region of *REG4* Gene

To analyze whether CDX2 directly binds to the putative CDX2-binding sites in the *REG4* 5′-flanking region, we performed chromatin immunoprecipitation (ChIP) assays using HSC-39 cells. Using 6 primers for the *REG4* 5′-flanking region (**Fig. 3A**), we recovered DNA fragments containing the *REG4* 5′-flanking region by primer 1, which encompasses presumptive CDX2-binding site C (**Fig. 3B**). DNA fragments from the 5′-flanking region of *REG4*, which were generated using primers 2, 3, 4, 5 and 6 such that they did not contain presumptive CDX2 binding sites, were not recovered by the anti-CDX2 antibody. The specificity of recovery of the *REG4* promoter region following ChIP with anti-CDX2

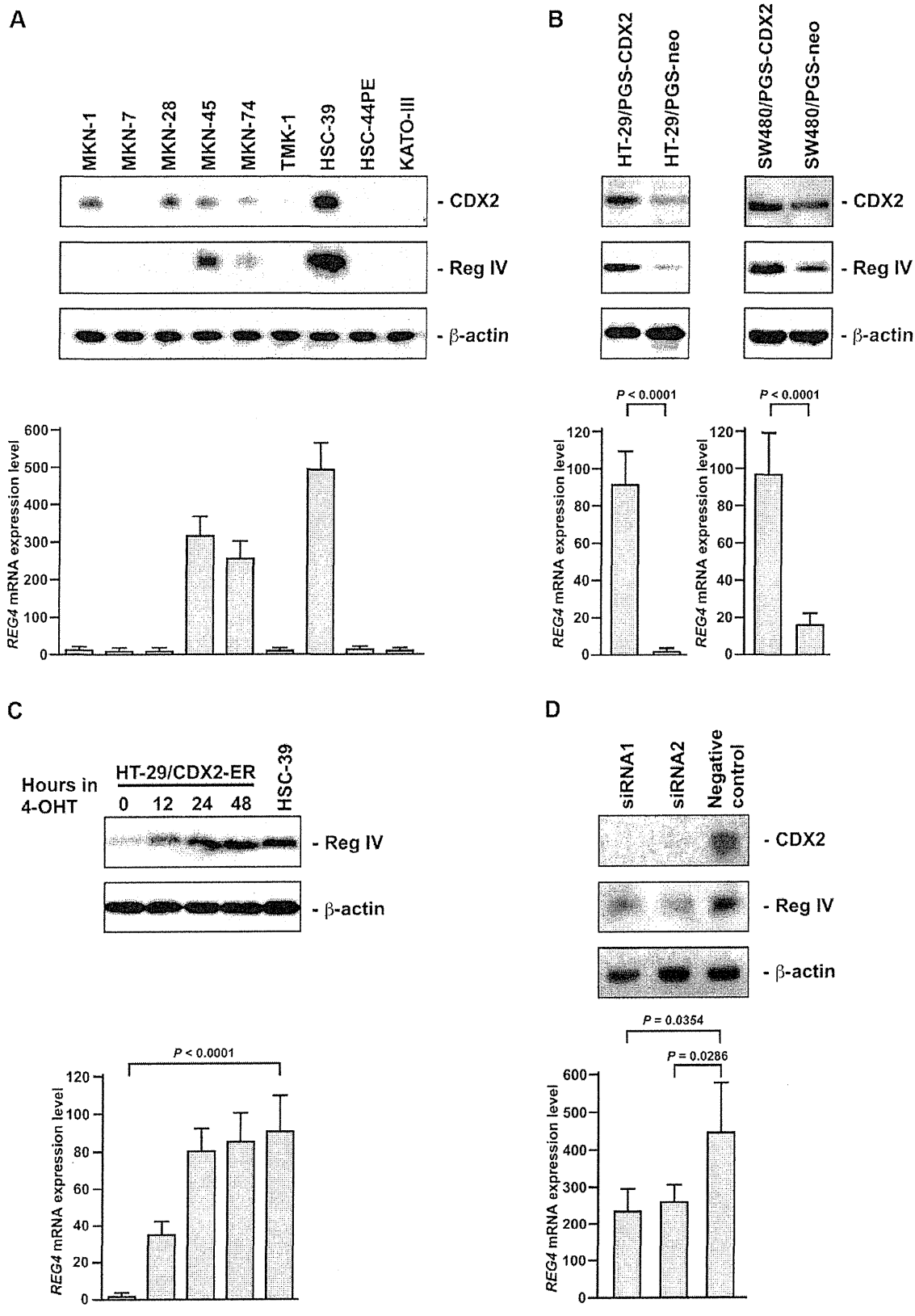
A
MKN-1
MKN-7
MKN-28
MKN-45
MKN-74
TMK-1
HSC-39
HSC-44PE
KATO-III
- CDX2
- Reg IV
- β-actin
REG4 mRNA expression level
B
HT-29/PGS-CDX2
HT-29/PGS-neo
SW480/PGS-CDX2
SW480/PGS-neo
- CDX2
- Reg IV
- β-actin
P < 0.0001
P < 0.0001
REG4 mRNA expression level
C
Hours in 4-OHT
HT-29/CDX2-ER
0 12 24 48
HSC-39
- Reg IV
- β-actin
P < 0.0001
REG4 mRNA expression level
D
siRNA1
siRNA2
Negative control
- CDX2
- Reg IV
- β-actin
P = 0.0354
P = 0.0286
REG4 mRNA expression level

Figure 1. Induction of Reg IV expression by CDX2. A: Western blot analysis of CDX2, Reg IV, and β-actin and qRT-PCR analysis of *REG4* in 9 GC cell lines. B: Western blot analysis of CDX2, Reg IV, and β-actin and qRT-PCR analysis of *REG4* in HT-29/PGS-CDX2, HT-29/PGS-neo, SW480/PGS-CDX2, and SW480/PGS-neo. C: Western blot analysis of Reg IV and β-actin and qRT-PCR analysis of *REG4* in HT-29/CDX2-ER. Time course of *REG4* gene induction in response to activation of a CDX2-ER fusion protein by 4-OHT was analyzed. D: Western blot analysis of CDX2, Reg IV, and β-actin and qRT-PCR analysis of *REG4* in HSC-39 cells transfected with CDX2 siRNA (siRNA1 and siRNA2) and the negative control siRNA. The units of *REG4* mRNA expression level are arbitrary. *P* values were calculated using Student's t-test. * N.S. = not significant.
doi:10.1371/journal.pone.0047545.g001

antibody was shown by the fact that other irrelevant DNA fragments lacking CDX2-binding sites (e.g., exon 3 of the *CDX1* gene) were not recovered (**Fig. 3B**). In addition, mock immunoprecipitation (mouse IgG) yielded few *REG4* or *CDX1*-specific DNA fragments (**Fig. 3B**). All these findings suggest that CDX2 activates *REG4* transcription by directly binding to sequences in the 5′-flanking region of the gene.

Trimethylation of Histone H3 Lysine 27 (H3K27me3) on the *REG4* Promoter in the GC Cell Lines

Although CDX2 protein expression was found in MKN-1 and MKN-28 cell lines, these 2 cell lines lacked detectable expression of *REG4* transcript and protein. Because it has been reported that DNA hypermethylation of CpG islands is associated with silencing of several genes [28], we investigate whether DNA methylation induced transcriptional inactivation of Reg IV in MKN-1 and MKN-28 cells. We treated these cells with a demethylating agent, 5-aza-2′-deoxycytidine (Aza-dC) and then performed qRT-PCR. However, Reg IV expression was not restored in these cell lines (**data not shown**), suggesting that DNA methylation is not likely to affect Reg IV expression. It has been also reported that H3K27me3 has been associated with repressed gene expression [29]. We further investigated H3K27me3 in GC cell lines. To determine the enrichment of H3K27me3 on the *REG4* promoter in the GC cell lines, ChIP assays were performed. In MKN-1 and MKN-28 cell lines, H3K27me3 levels on the *REG4* promoter region were high, whereas in HSC-39 cell line, H3K27me3 level on the *REG4* promoter region was low (**Fig. 3C**). These results suggest that closed chromatin structure of *REG4* promoter can inhibit Reg IV expression by CDX2.

Discussion

Although it has been reported that Reg IV expression is induced by GLI1 [21] or EGF [22], these molecules are unlikely to account for the association between Reg IV and intestinal differentiation. In the present study, we showed that endogenous CDX2 and Reg IV expression were well correlated in GC cell lines. In addition, using an ER-regulated form of CDX2, we found that there was rapid induction of Reg IV expression after 4-OHT treatment. Reporter gene assays revealed an important role for consensus CDX2 DNA binding elements in the *REG4* promoter region in its transcription. Subsequent ChIP assays showed that CDX2 binds directly to the *REG4* promoter. We previously showed that in primary GC tissue and intestinal metaplasia of the stomach, CDX2 and Reg IV expression were well correlated [11]. These results indicate that CDX2 protein directly regulates Reg IV expression in GC and intestinal metaplasia of the stomach.

CDX2 is overexpressed in intestinal phenotype GC and in intestinal metaplasia of the stomach [9,25]. In contrast, loss of CDX2 expression was observed in a subset of primary colorectal cancers, usually in poorly differentiated colorectal cancers [30]. The significance of alteration of CDX2 expression in human cancers remains unclear, and therefore it is important to define the target genes which are downstream of CDX2. We have identified several CDX2-regulated genes such as *CDH17* (which encodes LI-cadherin) [24], *HEPH* (which encodes hephaestin) [31], *ABCB1* (which encodes multidrug resistance 1) [32], and *DSC2* (which encodes desmocollin 2) [33]. Among these genes, *ABCB1* was originally identified as an overexpressed and amplified gene in multiple drug-resistant cells, and its product, P-glycoprotein, seems to play a critical role in drug resistance [34]. Previously, we reported that forced expression of Reg IV in GC cells inhibited 5-FU-induced apoptosis through induction of Bcl-2 and dihydropyrimidine dehydrogenase [8]. Taken together, it is possible that in intestinal phenotype GC, expression (or ectopic expression) of CDX2 induces Reg IV and multidrug resistance 1 expression, resulting in an increase in drug-resistance. In fact, it has been reported that postoperative chemotherapy is not beneficial for patients with intestinal phenotype GC [35].

Although our data support the view that CDX2 plays a role in regulating *REG4* transcription via binding to the promoter region, several findings indicate that CDX2 alone is not sufficient for activating *REG4* expression. In the present study, we generated a polyclonal population of MKN-7, TMK-1, HSC-44PE, and KATO-III cells which express high levels of CDX2 by infection with retroviruses carrying a full-length human CDX2 cDNA. However, overexpression of CDX2 failed to activate Reg IV expression. In GC cell lines, none of the cell lines with undetectable CDX2 protein expression had detectable *REG4* transcripts and protein. Therefore, CDX2 is required for Reg IV expression, but CDX2 alone is not sufficient for activating Reg IV expression. In the present study, nine GC cell lines were studied. The origins of the cell lines were as follows. The MKN-7, MKN-28, and MKN-74 cell lines were established from intestinal type GC. The TMK-1 and MKN-45 cell lines were established from diffuse type GC. The KATO-III, HSC-39, and HSC-44PE cell lines were established from signet ring cell carcinoma. The MKN-1 cell line was established from adenosquamous cell carcinoma. Because in intestinal metaplasia of the stomach, CDX2 and Reg IV expression are well correlated, GC cell lines established from diffuse type GC or signet ring cell carcinoma may not be suitable for the analysis of Reg IV induction by CDX2. In fact, Reg IV expression can be induced by CDX2 in cell lines derived from colon cancer in the present study. Furthermore, we showed that H3K27me3 levels on the *REG4* promoter region were high in MKN-1 and MKN-28 GC cell lines. These 2 cell lines lacked detectable expression of *REG4* although CDX2 protein expression was found. Therefore, H3K27me3 levels on the *REG4* promoter region may be high in MKN-7, TMK-1, HSC-44PE, and KATO-III cells, in which overexpression of CDX2 failed to activate Reg IV expression.

It has been reported that *REG4* mRNA expression was enhanced by stimulation with TGF-α, EGF, HGF, or bFGF through activation of the mitogen-activated protein kinase (MAPK) pathway [22]. Thus, it could be hypothesized that Reg IV is also regulated by downstream transcriptional factors of MAPK pathways. We performed *in silico* analyses of the *REG4* gene 5′-flanking region, and found at least one presumptive AP-1 consensus sequences (at −883 base pairs of *REG4* gene 5′-flanking region), which is a downstream transcriptional factor of MAPK signalling. In the present study, HSC-39 cells showed similar